 SL, vol.4, no.1, pp.31-38, 2010

Simulation of C-Start and S-Start of Fishes by an ALE-GFD Method and a Curvature-Wave Backbone Model

Y. Zhao[1], K.S. Yeo[1], P. Yu[1] and S.J. Ang[1]

Abstract: This paper presents the application of an Arbitrary Lagrangian Eulerian (ALE) and Singular Value Decomposition (SVD) based Generalized Finite Difference (GFD) method to simulate the C- and S-starts of a carangiform-type fish. The numerical model incorporate fluid-structure interaction (FSI) and computation is carried out on a hybrid grid comprising meshfree nodes around the undulating/deforming swimming fish and Cartesian nodes in the background. The meshfree nodes convect with the deformation and motion of the swimmer. A curvature-wave model of the backbone is used to generate the C- and S-start actions of the fish from the experimental data of Spierts and Leeuwen (1999). The curvature model provides a power tool to describe complex deformations of the fish backbone. The present study is probably the first to apply a curvature approach to reproduce the elegant and realistic manoeuvring kinematic actions of a carangiform-type fish.

Keywords: ALE-SVD-GFD, fish swimming, C-start, S-start, Curvature wave model, fluid structure interaction.

1 ALE-SVD-GFD

The Arbitrary-Lagrangian-Eulerian (ALE) form of the continuity and Navier Stokes (NS) equation satisfying the geometric conservation law (GCL) is given as [Farhat (2001)]:

$$\nabla \cdot \mathbf{u}=0 \tag{1}$$

$$\frac{\partial \mathbf{u}}{\partial \mathrm{t}} = -(\mathbf{u}-\mathbf{u^g}) \cdot \nabla \mathbf{u} + \frac{1}{\mathrm{Re}} \nabla \cdot \nabla \varepsilon(\mathbf{u}) - \nabla \mathrm{p} \tag{2}$$

where $\mathbf{u^g}$ is the node convection velocity and $\varepsilon(\mathbf{u}) = \nabla \mathbf{u} + (\nabla \mathbf{u})^{\mathbf{T}}$ is the strain rate tensor. Figure 1 shows the node categorization for the hybrid meshfree-Cartesian

[1] Department of Mechanical Engineering, National University of Singapore, 9 Engineering Drive 1, Singapore 117576

grid. Standard finite difference is applied at the category 1 background Cartesian nodes for spatial derivatives. Based on SVD (singular value decomposition) and multidimensional Taylor series expansion, the generalized finite difference (GFD) scheme is formulated for spatial derivative approximation on mesh free cloud nodes and category 3 Cartesian nodes. For 2D problems, minimum 9 supporting nodes are required to determine the spatial derivative of the central node to second order accuracy. The Taylor series expansion of n supporting nodes about the central node (see Figure 2) form a matrix equation

$$[\triangle \mathbf{f}]_{\mathbf{n}\times\mathbf{1}} = [\mathbf{S}]_{\mathbf{n}\times\mathbf{5}}[\partial \mathbf{f}]_{\mathbf{5}\times\mathbf{1}} \tag{3}$$

where $[\triangle \mathbf{f}]_{\mathbf{n}\times\mathbf{1}} = [f_1-f_0, f_2-f_0, \cdots, f_n-f_0]^{\mathbf{T}}$, $[\partial \mathbf{f}]_{\mathbf{5}\times\mathbf{1}} = [\frac{\partial f_0}{\partial x}, \frac{\partial f_0}{\partial y}, \frac{\partial^2 f_0}{\partial x^2}, \frac{\partial^2 f_0}{\partial y^2}, \frac{\partial^2 f_0}{\partial x \partial y}]^{\mathbf{T}}$,

$$[\mathbf{S}]_{\mathbf{n}\times\mathbf{5}} = \begin{bmatrix} \triangle x_1 & \triangle y_1 & 0.5\triangle x_1^2 & 0.5\triangle y_1^2 & \triangle x_1 \triangle y_1 \\ \triangle x_2 & \triangle y_2 & 0.5\triangle x_2^2 & 0.5\triangle y_2^2 & \triangle x_2 \triangle y_2 \\ \triangle x_3 & \triangle y_3 & 0.5\triangle x_3^2 & 0.5\triangle y_3^2 & \triangle x_3 \triangle y_3 \\ \vdots & \vdots & \vdots & \vdots & \vdots \\ \triangle x_n & \triangle y_n & 0.5\triangle x_n^2 & 0.5\triangle y_n^2 & \triangle x_n \triangle y_n \end{bmatrix}.$$

The derivative approximation at the central node is solved as

$$[\partial \mathbf{f}]_{\mathbf{5}\times\mathbf{1}} = [\mathbf{S}]^{+}_{\mathbf{n}\times\mathbf{5}}[\triangle \mathbf{f}]_{\mathbf{n}\times\mathbf{1}} \tag{4}$$

where $[\mathbf{S}]^{+}_{\mathbf{n}\times\mathbf{5}}$ is the pseudo inverse of $[\mathbf{S}]_{\mathbf{n}\times\mathbf{5}}$ obtained from SVD. The SVD-GFD scheme on fully meshfree grid systems is significantly more expensive than the standard FD approximation. However, the numerical efficiency is high for the current hybrid meshfree-Cartesian grid because the mesh free nodes occupy less than 5% of the total nodes. Besides, the hybrid meshfree-Cartesian grid provides important geometric flexibility for moving body and large deformations in complex domain compared with finite volume and finite element methods. The spatial temporal solution of the NS equation is second order accurate in accordance with the Crank-Nicolson based projection time scheme and the SVD-GFD approximation that is applied to the spatial derivatives. More details on ALE-GFD scheme may be found in Chew, Yeo and Shu (2006).

2 Curvature-wave model of the fish backbone

The cyclic swimming of carrangiform and subcarangiform fishes may generally be described in terms of the propagation of sinusoidal body waves of increasing amplitude from anterior to posterior according to Wu (1971). Liu (1996) and many researchers have modeled the undulating backbone of swimming fishes with the

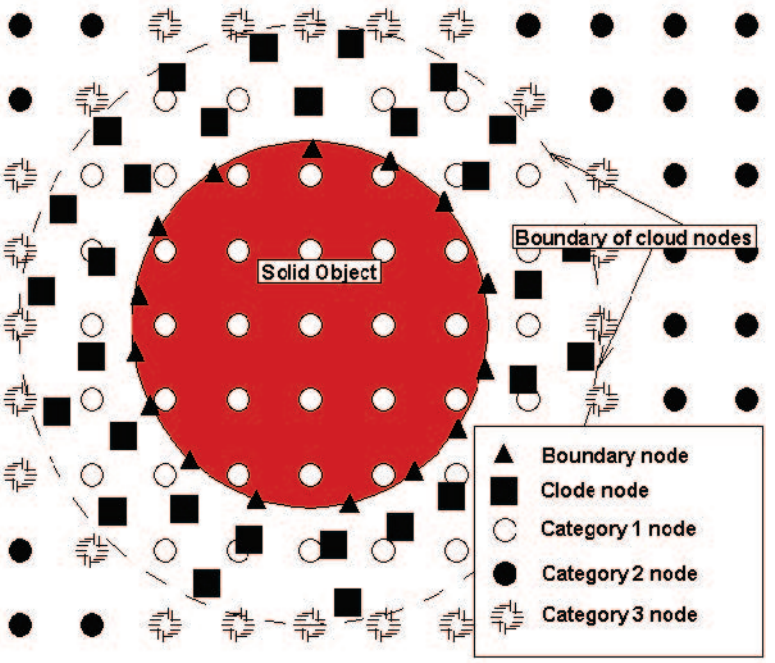

Figure 1: Terminology for hybrid meshfree-Cartesian grid system

following travelling wave equation $h(x,t) = a(x) \cdot \sin?(2\pi\left(\frac{x}{} - \frac{t}{T}\right))$, where represents the lateral wave amplitude, x is the lengthwise coordinate, t is the time step, is the wavelength and T is the period of undulation. This approach serves well for normal cruise swimming, but becomes highly cumbersome when describing the complex configurations of the fish backbone during sharp turning manoeuvres. In this study, the time-dependent configuration $\{x(l,t), y(l,t)\}$ of the fish backbone is derived by integrating the curvature equation:

$$\frac{d}{dl}(\theta, x, y) = (C(l;;t), cos\theta, sin\theta)(0 \leq l \leq 1), \tag{5}$$

where $C(l,t)$ is the time-dependent distribution of curvature along the intrinsic length l of the fish's backbone, and θ is the local angle of the backbone relative to its initial straight configuration. For a constant curvature of $C = 2\pi$, the fish will curl to form a perfect circle. The curvature model also exactly preserves the intrinsic length of the fish, which the simple sinusoidal wave model does not. In the present study, the curvature model (5) is used to generate realistic body actions of a carangiform fish model in C-start and S-start manoeuvres, using backbone curvature data recorded by Spierts and Leeuwen (1999) in their experiments. The

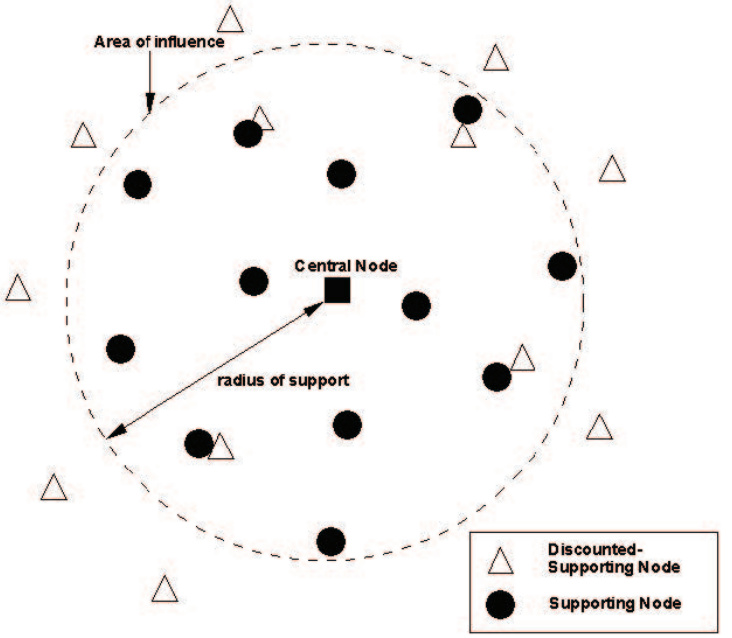

Figure 2: Terminology for GFD

experimental curvature data for C-Start and S-Start are fitted by bivariate spline functions to give $C(l,t)$, and equation (4) is integrated by the 4^{th}-order Runge-Kutta method. Equation (4) can also be applied for simple cruise swimming when $C(l,t)$ is prescribed by a sinusoidal travelling wave function. The curvature model can be further generalized for 3D fish to allow for torsion of the body along the backbone via the well-known Frenet's formula [Kreyszig (1991)].

2.1 Fish C-Start

The C-Start takes 1.5 non-dimension time units in the present simulation. The backbone motion is shown in the **Figure 3**. For the first 0.25 time unit, the fish sweeps its tail to its right and bends its body into a C-shape. At T=0.25, the body attains its maximum curvature at the position 0.625L from the head. This corresponds to the upstroke period. The next 0.5 time unit is the downstroke period, where the fish sweeps its tail back and straightens its body. The bulk of the C-start action thus occupies the first 0.75 time unit, which is underpinned by strong inertial flow effects. During this time the fish accomplishes most of its rotation. By T=0.75, the body is nearly straight. The body is allowed to straighten itself fully in the remaining 0.75

time unit in the present simulation, bringing the total time to 1.5 time units.

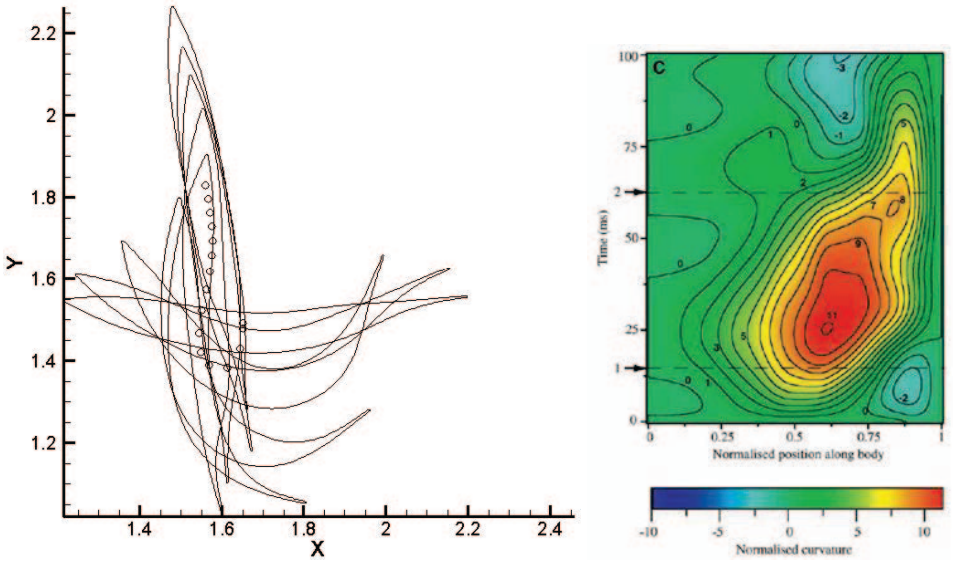

Figure 3: (a) Fish deformation and motion for C-Start at Re=2000, where the circles represent the center of mass (COM). (b) Fish backbone curvature contour over one non-dimensional time unit [from Spierts and Leeuwen (1999)].

Figure 4 shows the development of the vorticity field and streamtraces during the C-Start. Due to non-symmetric bending action of the fish body, there is uneven distribution of vorticity along the fish in (a). The attached vortices in the near field give a strong thrust in the rear section of the fish causing it to rotate sharply clockwise in (b). The starting vortices created at upstroke are shed from the head and tail to form a positive vortex on the left and a negative vortex on the right of the fish respectively in (c). The other vortices are shed during the downstroke period and later times. The strongest and second strongest positive vortices are formed along the convex side of the fish during the upstroke period and these are shed during the early downstroke period. They are subsequently paried with negative vortices shed from the concave side of the fish to form a vortex pair in the wake region of the fish in the post-C period in (c). The fish turns right through a resultant angle of 85.6 degree in this C-start sequence. The streamtraces (d)-(f) present an equivalent picture of flow development around the fish, with clearer details of the evolving velocity field.

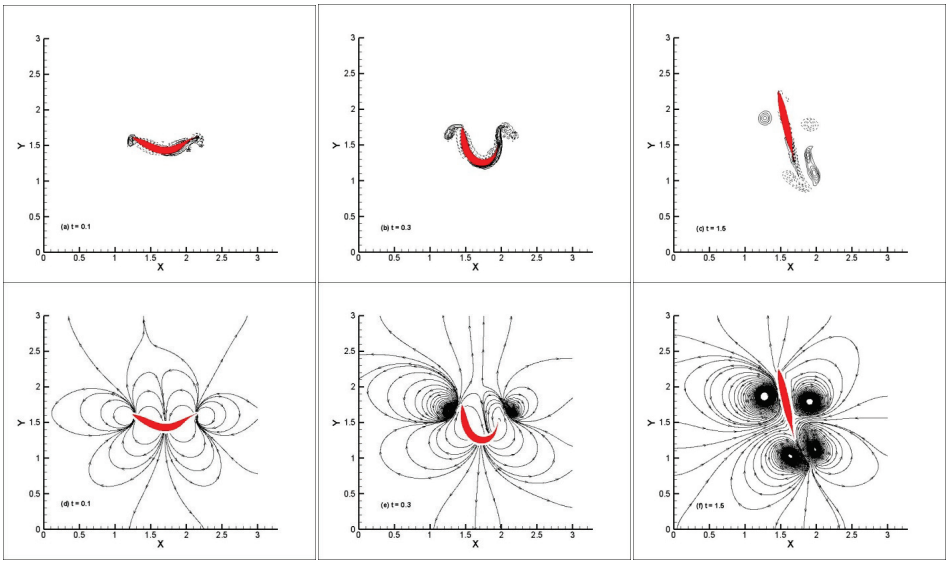

Figure 4: (a)-(c) depicts the vorticity fields and (d)-(f) the streamtraces fields at times 0.1, 0.3 and 1.5 for C-start.

2.2 Fish S-Start

The complete S-start simulation occupies 1.625 dimensionless time units in the current study. **Figure 5** depicts the backbone action of fish. The fish initially bends its middle body downward (positive curvature). This positive curvature wave propagates from head to tail between 0.0 and 0.625. From time 0.125, a negative curvature wave begins to form in the anterior half of the fish and to propagate rearward at about the same speed as the positive wave. The positive and negative curvature waves coexist to give the fish an S shape up till the time of about 0.625. From time 0.5, a second but weaker positive curvature wave begins to form and to propagate rearward. It coexists with the earlier negative curvature wave to give a reduced S shape to the fish till the time of about 1.0, by which time the negative curvature have passed beyond the tail. At about this time a weak negative curvature wave may be seen to develop near the middle of the fish. This propagates past the tail by time of about 1.625 when simulation was halted.

The first negative curvature wave gives the fish a strongly arched body at time 0.4 in **Figure 6** (a). The first positive curvature wave peak leaving the body at the tail causes the shedding of the first positive vortex in (a). Similarly, the negative curvature wave peak leaving at the tail at time 0.8 causes the shedding of the first

(a) (b)

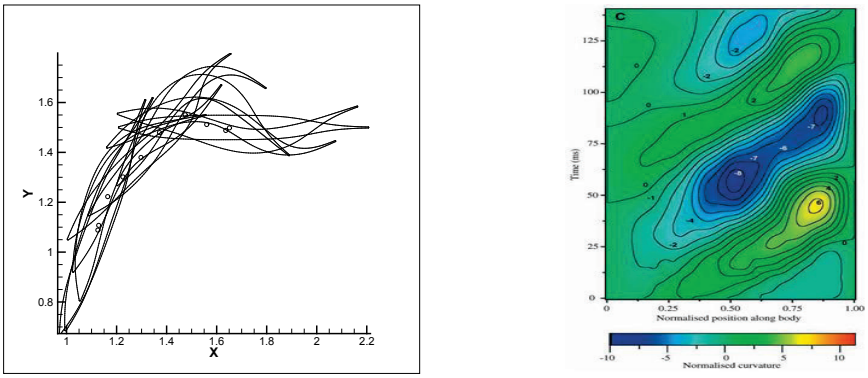

Figure 5: (a) Fish deformation and motion for S-start at Re=2000, where the circles represent the center of mass (COM). (b) Fish backbone curvature contour from Spierts and Leeuwen (1999).

negative vortex in the wake. The vorticity in these vortices is derived from the left and right side of the fish body respectively. The departure of the subsequent curvature waves as the body regains its straightened form leads to the further vortex shedding. Negative curvature waves dominate over the positive ones. The stronger negative shedded vortices cause the shedded vortex system to tilt clockwise. The fish turns left through a resultant angle of 79.5 degrees in this S-start manoeuvre. Figures 6(d-f) depict corresponding streamtraces field.

3 Conclusions

In this paper an ALE-SVD-GFD numerical scheme on hybrid meshfree-Cartesian spatial grid is applied to simulate C- and S-start manoeuvres of a carangiform type fish. The body actions of the fish are prescribed via a curvature-wave model of the backbone. The motion of the fish is derived from dynamical interaction between the deforming fish body and the surrounding fluid. Examples of elegant and realistic looking C- and S-start manoeuvres are presented using experimental backbone curvature data from Spierts and Leeuwen (1999). The present study shows that the curvature wave model is an effective methodology for generating complex self-propulsion and manoeuvring actions of fishes.

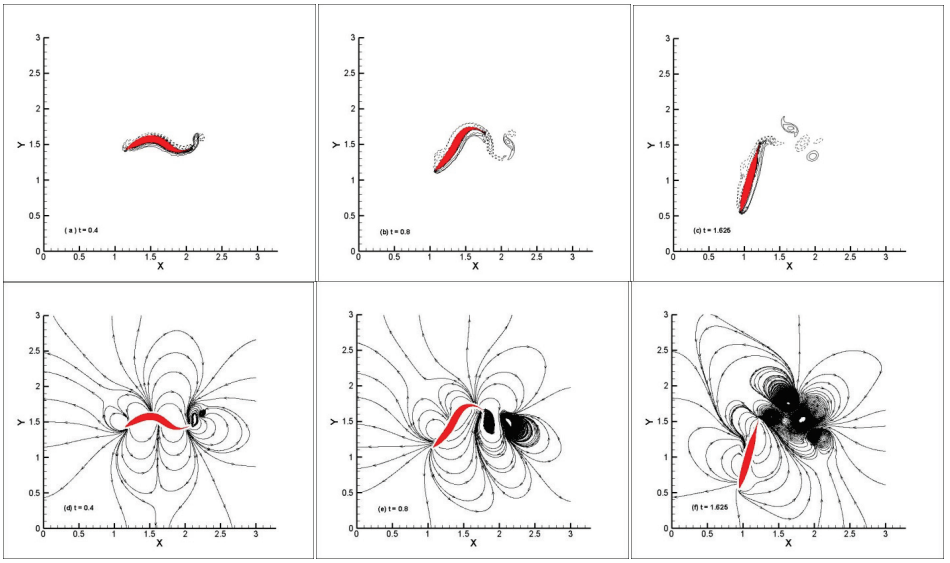

Figure 6: (a)-(c) depicts the vorticity fields and (d)-(f) the streamtraces fields at times 0.4, 0.8 and 1.625 for S-start.

References

Chew, C.S.; Yeo, K.S.; Shu, C. (2006): A generalized finite-difference (GFD) ALE scheme for incompressible flows around moving solid bodies on hybrid meshfree-Cartesian grids. *J.Comp.Phys.*, 218, pp. 510-548.

Farhat, C.; Geuzaine, P.; Grandmont, C. (2001): The discrete geometric conservation law and the nonlinear stability of ALE schemes for the solution of flow problems on moving grids. *J.Comp.Phys.*, 174, pp. 669-694.

Kreyszig, E. (1991): Formulae of Frenet. §15 in Differential Geometry. New York: Dover, pp. 40-43.

Liu, H.; Wassersug, R.J.; Kawachi, K. (1996): A computational fluid dynamics study of tadpole swimming. *J.Exp.Bio.*, vol. 199, pp. 1245-1260.

Spierts, I. L.Y.; van Leeuwen, J.L. (1999): Kinematics and muscle dynamics of C- and S-Starts of Carp. *J.Exp.Bio.*, vol. 202, 393-406.

Wu, T.Y. (1971): Hydromechanics of swimming fishes and cetaceans. *Adv. Appl. Mech.*, vol.II, pp. 1-63.